Supplemental Information

Dose discrimination in single cells exposed to cytokines

Qiuhong Zhang, Sanjana Gupta, David L. Schipper, Gabriel Kowalczyk, Allison E. Mancini, James R. Faeder, Robin E. C. Lee

SUPPLEMENTAL CONTENTS

A

Model 1: Switch-like response

$$Response = \eta_{basal} + H(dose) \times SF_1 \times CellState \times \eta_{induced}$$

Model 2: Graded response

$$Response = \eta_{basal} + dose \times SF_2 \times CellState \times \eta_{induced}$$

Model 3: Graded response with threshold

$$Response = \eta_{basal} + H(dose) \times dose \times SF_3 \times CellState \times \eta_{induced}$$

$$H(dose) \equiv \begin{cases} 0, dose \leq thresh \\ 1, dose > thresh \end{cases}$$

B

Parameter	Value	Description
η_{basal}	0-5	Adds a random value to cellular responses to simulate basal noise and cell-to-cell heterogeneity
$\eta_{induced}$	±0-15%	Random fluctuations were incorporated into the dose-dependent response of each cell to simulate biological noise
dose	[0, 1, 2, 3]	Each model was simulated with 4 integer doses, with '0' representing the untreated condition
SF_1	6	Scaling factor for Model 1 to normalize responses between models
SF_2	1.5	Scaling factor for Model 2
SF_3	2	Scaling factor for Model 3
CellState	[1,2,…,100]	Each cell was initialized with a unique integer value to describe its state
thresh	0-4	Each cell was initialized with a random value to describe its threshold for activation (used with *H(dose)* in models 1 and 3)

Figure S1, related to main figure 1. Description for 3 models of single cell dose responses. (A) Formulae for (M1) Switch-like, (M2) Graded, and (M3) Graded with threshold (top, middle and bottom respectively) models of single cell responses. M1 and M3 differ from M2 because they incorporate a heavyside function to model a switch-like behavior. For all models 100 cells were simulated, each initialized with a unique integer value between 1 and 100 to approximate heterogeneity in the cellular state. During initialization each cell was also assigned a threshold for activation (thresh) used in models M1 and M3 to determine whether a cell responds to a given dose. In all models, the strength of response to a dose of cytokine scales linearly with the cell's state, whereby a cell with state 100 and a cell with state 0 will have the strongest and weakest responses respectively. **(B)** Parameter values used for simulations described in (A) as well as Figure 1 of the main text. Basal noise (η_{basal}) was used as a cut-off to quantify the non-responsive fraction in the right column of Figure 1B. That is, non-responders are defined as: $Response \leq (\eta_{basal})_{MAX}$.

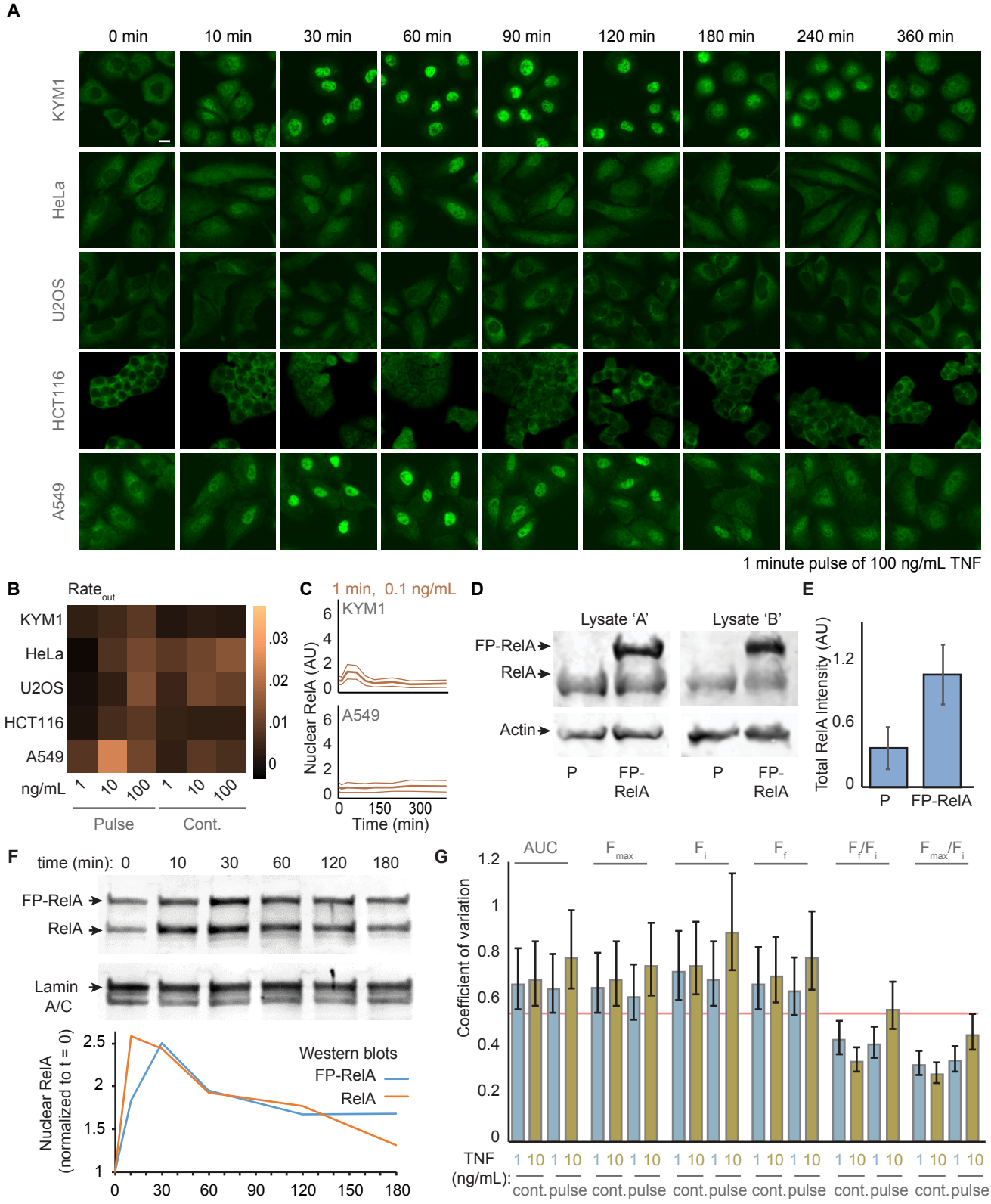
A
0 min
10 min
30 min
60 min
90 min
120 min
180 min
240 min
360 min
KYM1
HeLa
U2OS
HCT116
A549
1 minute pulse of 100 ng/mL TNF
B
Rate out
KYM1
HeLa
U2OS
HCT116
A549
ng/mL
1
10
100
1
10
100
Pulse
Cont.
.03
.02
.01
0
C
1 min, 0.1 ng/mL
KYM1
A549
Nuclear RelA (AU)
Time (min)
D
Lysate 'A'
Lysate 'B'
FP-RelA
RelA
Actin
P
FP-RelA
P
FP-RelA
E
Total RelA Intensity (AU)
P
FP-RelA
F
time (min): 0 10 30 60 120 180
FP-RelA
RelA
Lamin A/C
Nuclear RelA (normalized to t = 0)
Western blots
FP-RelA
RelA
G
AUC
F max
F i
F f
F f/F i
F max/F i
Coefficient of variation
TNF (ng/mL):
cont. pulse

Figure S2, related to main figure 2. Subcellular localization of endogenous RelA in human cancer cells. (A) Fixed-cell RelA immunofluorescence images of KYM1, HeLa, U2OS, HCT116, and A549 cells. Cells were treated with a 1 minute pulse of 100 ng/mL of TNF and fixed at the indicated time after cytokine exposure; scale bar 10 μm. **(B)** Heatmap for $Rate_{out}$ descriptor does not show a significant trend. **(C)** KYM1 cells show greater sensitivity to low concentrations of TNF when compared with A549 cells, the second most responsive cell line to TNF. **(D)** Western blot of RelA in lysates from parental KYM1 cells (P) and KYM1 cells that express mVenus-RelA (FP-RelA). Biological replicates are shown. **(E)** Quantification of bands from (D) show that FP-RelA is overexpressed 2.9-fold when compared with P KYM1 cells. For FP-RelA, endogenous and FP-RelA bands were summed; ±SEM. **(F)** Western blot of nuclear lysates (top) from FP-RelA cells collected at indicated times after exposure to a 1 minute pulse of 10 ng/mL TNF. Quantification of endogenous and FP-RelA bands (bottom) show qualitatively similar dynamics to each other. **(G)** Bar graphs of the coefficients for variation for descriptors (described in Figure 2B) of nuclear FP-RelA density in cells exposed to TNF conditions as indicated. Error bars represent 95% confidence interval of the coefficient of variation.

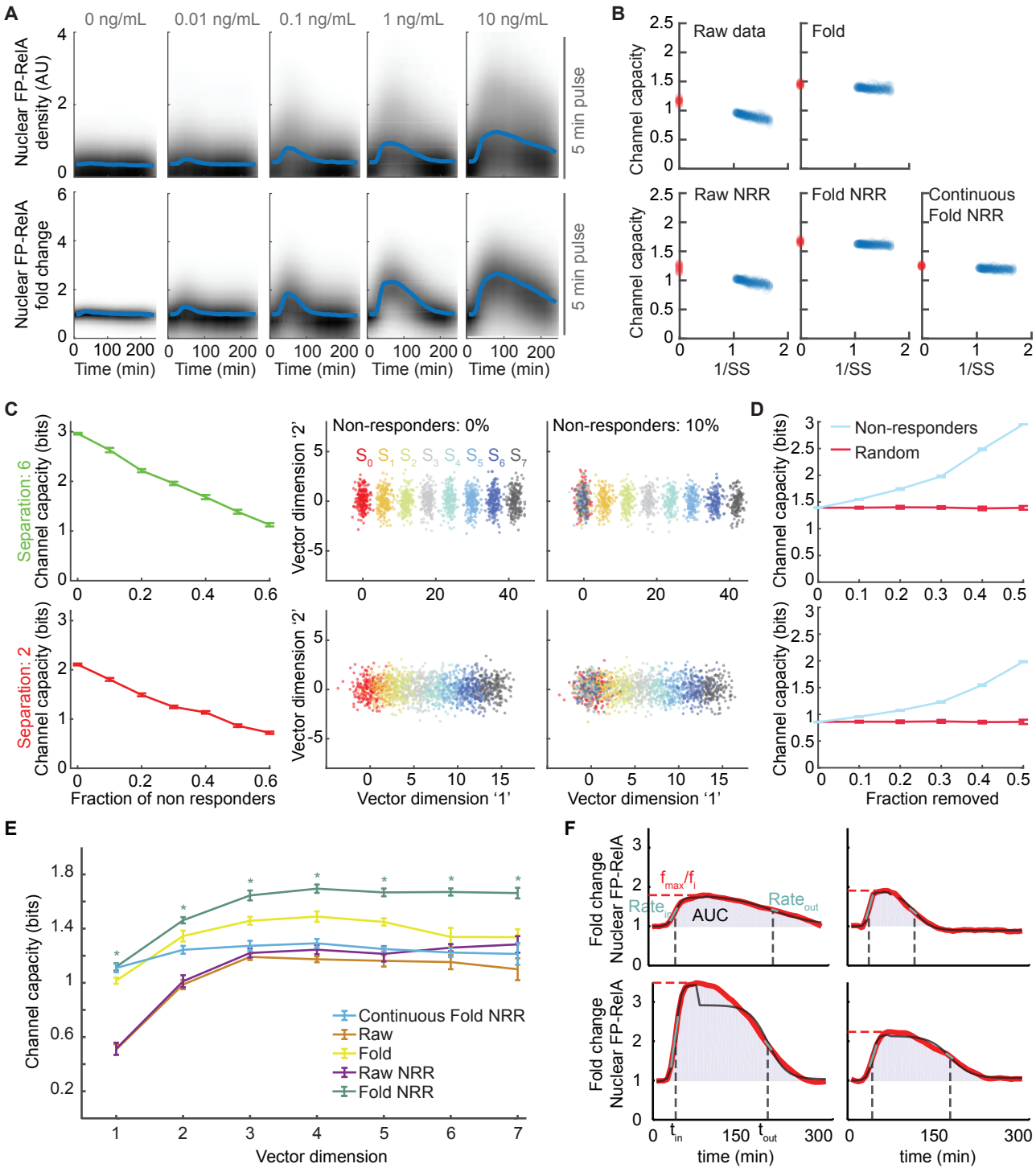
A
0 ng/mL
0.01 ng/mL
0.1 ng/mL
1 ng/mL
10 ng/mL
Nuclear FP-RelA density (AU)
Nuclear FP-RelA fold change
5 min pulse
Time (min)
B
Raw data
Fold
Raw NRR
Fold NRR
Continuous Fold NRR
Channel capacity
1/SS
C
Separation: 6
Separation: 2
Channel capacity (bits)
Fraction of non responders
Non-responders: 0%
Non-responders: 10%
Vector dimension '2'
Vector dimension '1'
D
Non-responders
Random
Fraction removed
E
Channel capacity (bits)
Vector dimension
Continuous Fold NRR
Raw
Fold
Raw NRR
Fold NRR
F
Fold change Nuclear FP-RelA
AUC
time (min)

Figure S3, related to main figure 3. Details of control analysis, models, and features used in channel capacity calculations. (A) Density plots for nuclear FP-RelA in KYM1 cells exposed to a 5 minute TNF pulse of indicated concentration. Raw trajectories (top) and fold-transformed trajectories (bottom) are shown with the untreated control sample in the left-most column. **(B)** Plots showing jackknife analysis for channel capacity calculations. To correct for sample size bias and determine the variance of channel capacity values, the data set was jackknifed at sequentially increasing fractions, SS (points shown in blue) followed by linear regression to extrapolate the channel capacity at a sample size of infinity (i.e. 1/SS = 0; points shown in red). The lines obtained via linear regression are relatively flat, indicating that the size of our dataset is large enough to accurately estimate the channel capacity. **(C)** Plots showing the degradation in channel capacity of a system of eight 2-D Gaussians, when subpopulations of non-responders are considered. Fully separated Gaussians show the theoretical maximum channel capacity of 3 bits for this system (middle top). Overlap in the Gaussians (middle bottom), or the presence of bimodal distributions with an overlapping basal population (right) significantly reduces the values of channel capacity calculations (left); k = 10; ± standard deviation. **(D)** The effects of subsampling were simulated for the Gaussian system described in (C), except starting with 50% of the population sampled from the basal distribution for fully separated Gaussians (top) or overlapping Gaussians (bottom). In contrast with randomly targeted removal (red), channel capacity values after selectively removing a defined fraction of non-responders (blue) increases the channel capacity up to the defined limit revealing the true channel capacity of the responsive subpopulation; ± standard deviation. **(E)** Channel capacity values calculated for each data set over a range of vector dimensions (d = 5 is reported in the manuscript): Single-cell trajectories for 'Raw' data sets are in arbitrary fluorescence units; for 'Fold' data sets, each single-cell time course is represented as fold change (A); for 'NRR' data sets, single-cell trajectories with < 1.2-fold change in nuclear FP-RelA are removed; the continuous data set only includes conditions with continuous exposure to TNF (bottom row of Figure 3A). Green stars compare Fold-NRR and Raw-NRR ($p < 10^{-6}$, t test). **(F)** Representative sigmoid fits of five single cell time courses. The red lines show representative experimental trajectories for a single cell's nuclear FP-RelA time course. Black lines show two sigmoid fits used to approximate phases of nuclear entry and exit for FP-RelA and to calculate t_{in} and t_{out}. $Rate_{in}$ and $Rate_{out}$ were calculated from the slopes of adjacent time points from the experimental trajectory (teal line segments). The region used to calculate the AUC is indicated by the shaded area.

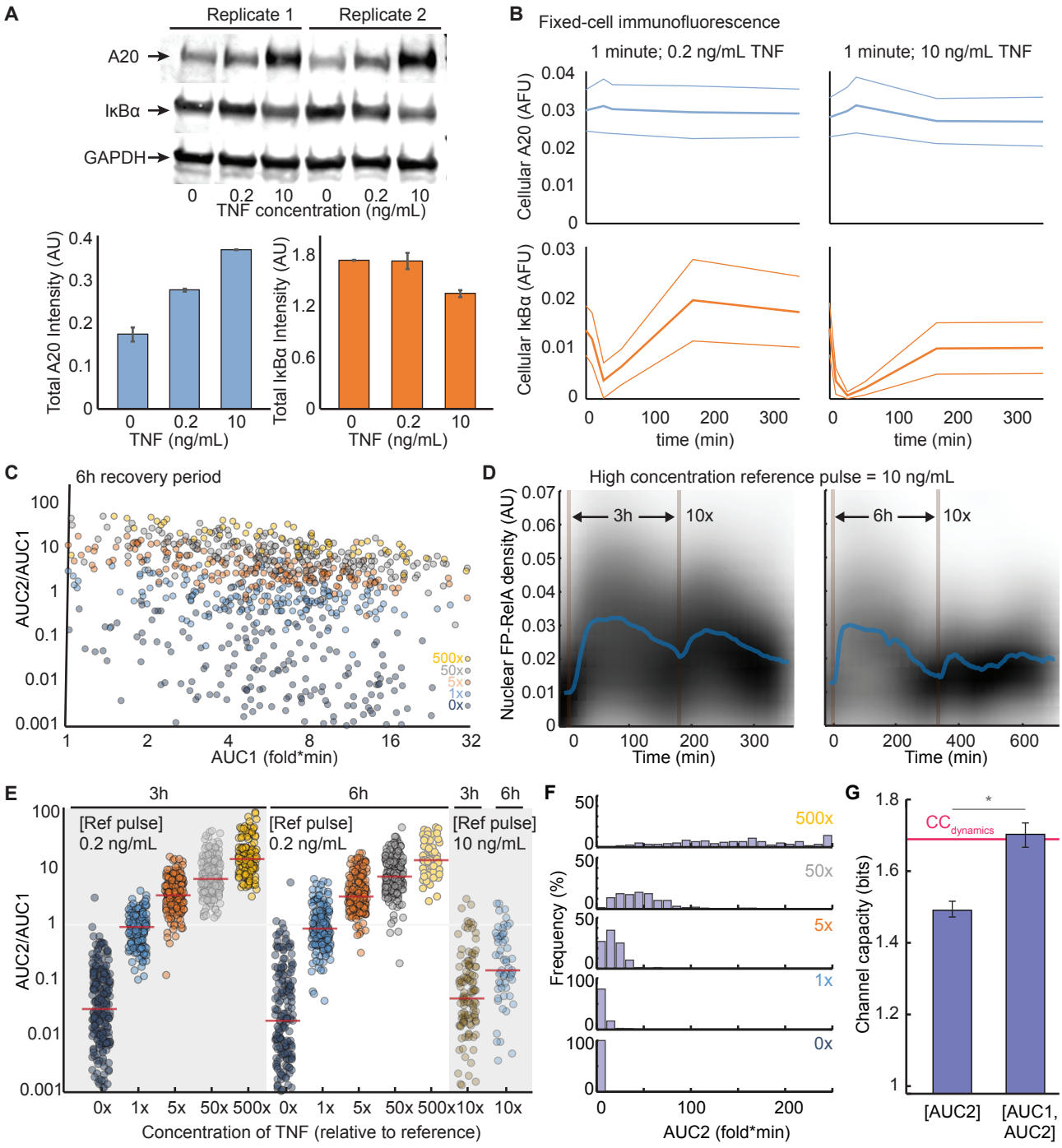
A
Replicate 1
Replicate 2
A20
IκBα
GAPDH
0 0.2 10 0 0.2 10
TNF concentration (ng/mL)
Total A20 Intensity (AU)
Total IκBα Intensity (AU)
TNF (ng/mL)
B
Fixed-cell immunofluorescence
1 minute; 0.2 ng/mL TNF
1 minute; 10 ng/mL TNF
Cellular A20 (AFU)
Cellular IκBα (AFU)
time (min)
C
6h recovery period
AUC2/AUC1
AUC1 (fold*min)
500x
50x
5x
1x
0x
D
High concentration reference pulse = 10 ng/mL
3h
10x
6h
10x
Nuclear FP-RelA density (AU)
Time (min)
E
3h
6h
3h
6h
[Ref pulse]
0.2 ng/mL
[Ref pulse]
0.2 ng/mL
[Ref pulse]
10 ng/mL
AUC2/AUC1
0x 1x 5x 50x 500x 0x 1x 5x 50x 500x 10x 10x
Concentration of TNF (relative to reference)
F
Frequency (%)
500x
50x
5x
1x
0x
AUC2 (fold*min)
G
CC dynamics
Channel capacity (bits)
[AUC2]
[AUC1, AUC2]
*

Figure S4 related to main figure 4. Negative feedback and dampened responses in cells exposed to a high concentration reference pulse of TNF. (A) Western blots (top) for regulators of negative feedback A20 and IκBα in KYM1 cells 3 hours after exposure to a 1 minute reference pulse of TNF at indicated concentration. GAPDH-normalized band intensities quantified in bar graphs (bottom) show that negative regulators are perturbed greater in response to a high concentration reference pulse (10 ng/mL) in comparison with a low concentration reference (0.2 ng/mL); ±SEM of biological duplicate. **(B)** Results from (A) are confirmed by time courses for average cellular A20 (left) and IκBα from fixed-cell immunofluorescence KYM1 exposed to indicated TNF conditions. Light colored lines indicate the standard deviation. **(C)** Scatter plots showing AUC2/AUC1 stratified along AUC1 across the range of test conditions in cells after a 6 hour recovery period. **(D)** Density plots of single-cell FP-RelA time courses for cells exposed to a high concentration (10 ng/mL) reference pulse of TNF followed by a TNF pulse with a 10x increase in concentration 3 hours (left) or 6 hours (right) later. **(E)** Jitter plots comparing AUC2/AUC1 responses in single cells exposed to a low concentration reference pulse (0.2 ng/mL) or a high concentration reference pulse (10 ng/mL) of TNF with either a 3 hour or 6 hour intervening recovery window. Responses to test pulses are significantly dampened when cells are exposed to a high concentration reference pulse regardless of the duration of the recovery window. **(F)** Frequency distributions of AUC2 across the range of test conditions. **(G)** Channel capacity values calculated using AUC2 are compared with a vector that includes reference information about each cell ([AUC1, AUC2]). Red line indicates the channel capacity calculated from the full matrix of conditions (Figure 3); ± standard deviation; $p < 10^{-11}$.

SUPPLEMENTAL MOVIE LEGENDS

Movie S1, related to main figure 2. TNF-induced nuclear translocation of FP-RelA in live KYM1 cells. Time course of nuclear translocation in live KYM1 cells exposed continuously to 1 ng/mL TNF.

Movie S2, related to main figure 4. Nuclear translocation of FP-RelA during repeat stimulation in live KYM1 cells. Time course of nuclear translocation in live KYM1 cells exposed first to a 1 minute 'reference pulse' of 0.2 ng/mL TNF, followed 3 hours later by a 1 minute 'test pulse' of 1 ng/mL TNF (i.e. a 5x increase in concentration).

SUPLEMENTAL TABLES

Table S1, related to main Figure 2. Summary of cell numbers for fixed cell experiments. For each condition cells were exposed continuously or to a pulse of cytokine, and fixed after 0, 10, 30, 60, 90, 120, 180, 240, or 360 minutes. 'Total' is the aggregate number of cells measured across all time points, 'Avg #' quantifies the average number of cells measured in each time point, and 'StDev' quantifies the standard deviation across time points for indicated condition.

	1 ng/ml	10 ng/ml	100 ng/ml	1 ng/ml	10 ng/ml	100 ng/ml
	Pulse	Pulse	Pulse	Continuous	Continuous	Continuous
	Total					
KYM1 TNF	8848	5390	8894	8981	8034	7376
HeLa TNF	4356	4312	3818	5371	4865	5077
U2OS TNF	8550	8280	8864	10706	10031	8856
HCT116 TNF	29243	23119	27174	33410	32012	29683
A549 TNF	3512	2882	9066	6354	5689	8490
	Avg #					
KYM1 TNF	983.11	598.89	988.22	997.89	892.67	819.56
HeLa TNF	484	479.11	424.22	596.78	540.56	564.11
U2OS TNF	950	920	984.89	1189.56	1114.56	984
HCT116 TNF	3249.22	2568.78	3019.33	3712.22	3556.89	3298.11
A549 TNF	390.22	320.22	1007.33	706	632.11	943.33
	StDev					
KYM1 TNF	120.48	103.66	167.87	230.21	321.18	370.25
HeLa TNF	22.51	19.73	52.29	30.35	39.4	46.64
U2OS TNF	295.58	152	241.88	333.66	343.66	172.45
HCT116 TNF	415.67	305.31	404.14	402.29	290.18	456.39
A549 TNF	67.44	42.29	129.58	133.76	84.9	177.26

Table S2. Related to main Figure 4. Summary of pairwise p-values for AUC2/AUC1 compared between test pulse conditions. For each pair of test pulse conditions in Figure 4D, p-values are lower than listed. Concentrations listed are relative to a test pulse concentration of 0.2 ng/mL TNF.

Test pulse	0x	1x	5x	50x	500x
0x	-	10^{-17}	10^{-36}	10^{-27}	10^{-22}
1x	10^{-17}	-	10^{-27}	10^{-24}	10^{-21}
5x	10^{-36}	10^{-27}	-	10^{-11}	10^{-16}
50x	10^{-27}	10^{-24}	10^{-11}	-	10^{-6}
500x	10^{-22}	10^{-21}	10^{-16}	10^{-6}	-